Analysis and design optimization of an integrated micropump-micromixer operated for bio-MEMS applications

Cesar A. CORTES-QUIROZ [1,*], Alireza AZARBADEGAN [2], Ian D. JOHNSTON [1], Mark C. TRACEY [1]

* Corresponding author: Tel.: +44 (0)1707 284147; Fax: +44 (0)1707 281306; Email: c.cortes-quiroz@herts.ac.uk
1: School of Engineering and Technology, University of Hertfordshire, UK
2: Department of Mechanical Engineering, University College London, UK

Abstract A generic microfluidic system composed by two single chamber valveless micropumps connected to a simple T-type channel intersection is examined numerically. The characteristics of a feasible valveless micropump have been used in the design, where efficient mixing is produced due to the pulsating flow generated by the micropumps. The advantages of using time pulsing inlet flows for enhancing mixing in channels have been harnessed through the activation of intrinsic characteristics of the pumps required to achieve the periodic flows.
A parametric study is carried out on this microfluidic system using Computational Fluids Dynamics (CFD) on a design space defined by a Design-of-Experiments (DOE) technique. The frequency f and the phase difference ϕ of the periodic fluid velocities (operation parameters) and the angle θ formed by the inlet channels at the intersection (geometric parameter) are used as design parameters, whereas mixing quality, pressure drop and maximum shear strain rate in the channel are the performance parameters. The study identifies design features for which the pressure drop and shear strain are reduced whereas the mixing quality is increased.
The proposed microfluidic system achieves high mixing quality with performance parameters that enable manipulation of biological fluids in microchannels.

Keywords: Microfluidics, Micropump-micromixer, Parallel Valveless Micropump, Pulsating Flow, Microsystem Design, Optimization

1. Introduction

Microfluidic systems for biological and chemical applications necessitate mixing of reagents as a routine protocol. Many biosensors require two fluids to be mixed prior to their introduction to specific sensors. The ability of a sensor to detect biomarkers depends on the mixing efficiency obtained in the integrated microsystem. However, mixing in the micrometre scale is marred by the low Reynolds number and thus by the laminar flow that only facilitates mixing based on molecular diffusion.
Several methods for microfluidic mixing have been reported, mostly based on geometry features, miniature stirrers, or external fields (electric, magnetic, ultrasonic) that decrease diffusion distance by rearranging the flow paths, inducing secondary flows or perturbing the laminar regime of the flow. Various strategies towards achieving efficient mixing in microfluidic devices have been reviewed (Hessel et al., 2005; Nguyen and Wu, 2005).
A technique that can enhance mixing between two reagents without using additional geometric features, miniature parts, or external fields, consists of introducing time pulsing cross-flows into a main channel from one or multiple perpendicular inlets to distort the interface between the reagents in the main channel (Niu and Lee, 2003). Similarly, mixing has been enhanced by varying periodically the flow rates in two perpendicularly intersected inlet channels (Glasgow and Aubry, 2003). Other studies have used periodic velocity perturbations to the species streams coming into the mixing channel with geometric structures downstream such as a wavy-wall section (Chen and Cho, 2008) or obstacles (Miranda et al., 2010).

Although these studies have demonstrated the advantages of using time pulsing inlet flows for enhancing mixing in microchannels, they implemented pulsating flows merely on the basis of theoretical sinusoidal equations for the inlet velocities of fluids and they did not refer to any characteristic of the micropumps that are required to achieve effective periodic flows in a truly integrated microsystem.

In this paper, a microfluidic system is presented and evaluated numerically. It is composed by two single-chamber parallel valveless micropumps connected to a simple T-type micromixer. Some characteristics of the pumps such as the actuator frequency f and the phase difference ϕ between them (operation parameters), plus the angle θ formed between the inlet channels at their junction to the mixing channel (geometric parameter) were used as system design parameters, whereas mixing quality, pressure drop and maximum shear strain rate in the channel were used as performance parameters. Several cases resulting from combining a discrete number of values of the design parameters using the Design of Experiments (DOE) technique enabled the analysis and identification of the designs giving higher mixing quality as well as lower pressure drop, shear strain rate and shear stress.

2. Microsystem design

The microfluidic system integrates two identical single chamber valveless micropumps arranged in parallel (Azarbadegan et al., 2010, 2013) with a typical T-type micromixer. Each pump drives one of the fluids to mix and their outlet channels become inlet channels of the micromixer. The mixing channel is the outlet channel of the system. Additional channels, chambers or structures in the mixing channel are not included. A schematic view of the microsystem is shown in Fig. 1.

The dimensions shown in Fig.1 have been fixed, with the height of microchannels equal to 70 μm in the whole system. The exception is the dimension θ which has been used as a design variable in the parametric study.

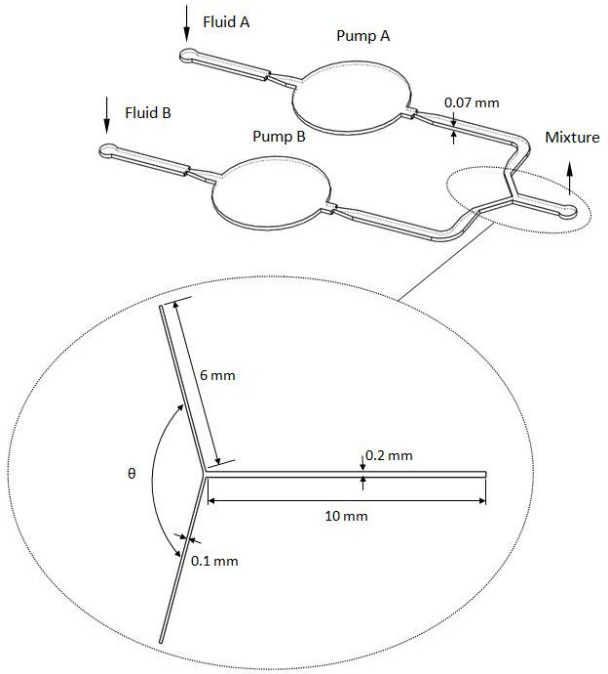

Fig. 1. Schematic of the microsystem with two parallel valveless micropumps and a T-type micromixer.

The configuration, operation characteristics and physical boundary conditions of the micropumps have been reported by Azarbadegan et al. (2010). Basically, the pump chambers are cylindrical cavities whose planar surfaces are forced vertically to deflect at an angular frequency $2\pi f$. The chambers are connected to two diffuser-nozzle structures. The volume displacement caused by the deformation of a disc centred on top of the chamber and the asymmetric pressure drop across the diffuser-nozzle elements with the flow direction, result in a rectified mean flow. The actuator frequency f and the forcing phase difference ϕ between them are in the range of 1 to 100 Hz and $\pi/36$ to π respectively.

3. Methodology

A numerical study of the microsystem performance was done on a set of design configurations described by a single geometric parameter and a set of realistic micropump operation parameters. A DOE technique was used to define these design cases.

3.1 Numerical simulations

Numerical simulations of the transport process in the microsystem are performed to

investigate the mixing quality that can be achieved in the geometrical configurations with different micropump operation conditions defined by the DOE (see section 3.2). The CFD code used for this study is the commercial Navier-Stokes Solver CFX 13.0 (ANSYS Inc., 2010) which is based on the Finite Volume Method. The geometries of the different configurations were modelled and meshed using the commercial mesh generator ICEM CFD 13.0 (ANSYS Inc., 2010).

A variable mesh composed of hexahedral elements is used and arranged to provide sufficient resolution for boundary layers near the fluid-solid interface on the walls of the channels. In order to obtain mesh-independent results from the simulations, a preliminary mesh size sensitivity study was carried out to determine the interval size of convergence.

The flow is defined viscous, isothermal, incompressible, laminar and in transient-state, for which equations of continuity (Eq. (1)), momentum (Eq. (2)) and species convection-diffusion (Eq. (3)) are solved.

$$\nabla V = 0 \tag{1}$$

$$\rho V \nabla V = -\nabla P + \mu \nabla^2 V \tag{2}$$

$$V \nabla c = D \nabla^2 c \tag{3}$$

where ρ and μ are the density and viscosity of the fluid respectively, V is the velocity vector, P is the pressure, c is the mass fraction or concentration of the fluid under analysis and D is the diffusion coefficient of the fluid in the other fluid. Advection terms in each equation are discretized with a second order differencing scheme which minimize numerical diffusion in the results. The simulations were defined to reach convergence when the normalized residual for the mass fraction fell below 1 x 10^{-5}.

The boundary condition at the inlet channels of the micromixer component (see magnified part in Fig. 1) for the velocity is a uniform parallel velocity profile in the direction of the bulk flow. The velocity values at inlets 1 and 2 have been obtained from the operational characteristics of the micropumps, which reproduce the sinusoidal functions: *u1 = Um+Ua*cos(2*pi*t*f)* and *u2 = Um+Ua*cos(2*pi*t*f+ϕ)* respectively, where t is time, *Um* = (0.00023070146 [m])**f* is the mean velocity and *Ua* = (0.00234990581 [m])**f* is the velocity amplitude.

On the walls, a non-slip boundary condition is used. At the outlet of the mixing channel, a constant pressure condition (gauge pressure P = 0) is applied.

Water at 25 ºC and a diluted generic biological fluid are the fluids used in the study. Therefore, the physical properties of the biofluid have been considered to be the same as that of water (density, ρ_{H_2O}= 997 kg/m3; dynamic viscosity, μ_{H_2O}= 8.899E-04 kg/m.s), while its diffusivity in water has been taken as typical D = 1.0E-10 m2/s. The boundary conditions for the species balance are mass fractions equal to 0 at the inlet where pure water is fed and equal to 1 at the inlet where the biofluid is fed.

To analyze and compare the performance of the design configurations under different operation conditions, the outputs from CFD code has been post-processed to measure relevant performance parameters, as they are mixing quality, pressure drop and maximum shear strain rate in the mixing channel. The mixing quality is measured by the Mixing index, *Mi* (Cortes-Quiroz, 2010), which calculates the level of mass concentration distribution on a section plane by

$$Mi = 1 - \sqrt{\frac{\int_A \left(c - \bar{c}\right)^2 \, \mathrm{d}A}{A \cdot \bar{c}\left(1 - \bar{c}\right)}} \tag{4}$$

where c is the local mass concentration on a cross-section plane, $\bar{c}$ is the averaged value of the concentration field on the plane and A is the area of the plane. *Mi* reaches a value of 0 for a complete segregated system and a value of 1 for the homogeneously mixed case.

The pressure drop in the mixing channel has been calculated by the difference between the area weighted average of total pressure on the outlet plane and on a cross section plane at the inlet of the mixing channel.

3.2 Design of Experiments. The Taguchi method

A DOE technique defines a subset of experiments (design points) from the design space, which is representative enough to evaluate the influence of designs parameters on performance parameters.

The Taguchi method (Taguchi, 1987) has been used in this study. It is based on Orthogonal Array (OA) of experiments and gives much reduced variance for the experiment with optimum settings of design parameters. These parameters are: pump actuator frequency (f), phase difference between the pump actuators (ϕ) and angle formed by the inlet channels (θ). Table 1 shows the values of design parameters with five levels each that correspond to those in the set of design cases defined by the DOE. These are given by the Taguchi's OA L_{25} shown in Table 2.

Table 1
Design parameters and levels

Parameter[a] / Level	**A.** f (s^-1)	**B.** ϕ (rad)	**C.** θ (degrees)
1	1.00	Pi/36	120
2	25.00	Pi/4	150
3	50.00	Pi/2	180
4	75.00	3/4 Pi	210
5	100.00	Pi	240

Table 2
Orthogonal array L_{25} (design matrix) for three parameters

Parameter[a] / Experiment[b]	**A**	**B**	**C**
1	1	1	1
2	1	2	2
3	1	3	3
4	1	4	4
5	1	5	5
6	2	1	2
7	2	2	3
8	2	3	4
9	2	4	5
10	2	5	1
11	3	1	3
12	3	2	4
13	3	3	5
14	3	4	1
15	3	5	2
16	4	1	4
17	4	2	5
18	4	3	1
19	4	4	2
20	4	5	3
21	5	1	5
22	5	2	1
23	5	3	2
24	5	4	3
25	5	5	4

[a] Parameters are defined in Table 1

[b] Experiments correspond to models of CFD simulations

4. Results and analysis

The numerical models implemented for the evaluation of the microsystem performance correspond to the 25 design cases of Table 2. They define five geometric configurations given by the values of parameter θ under different micropump operation conditions given by the values of parameters f and ϕ (see Table 1). In this section, the results of the numerical simulations are presented for different performance variables. These results correspond to the last time step (total time) of the transient simulations. With the total time set as ttot = 100/f [s], i.e., 100 cycles of the micropump actuators, and the time step as tstep = 1/(100*f) [s], the simulation times go from 1 s (f = 100 Hz) to 100 s (f = 1 Hz), with corresponding time steps of 0.0001 and 0.01 s respectively. The chosen time steps ensure that the simulations capture properly the variation of the flow physics inside the system and converge correctly with 10000 time steps per simulation.

The results of mixing index are shown in Fig. 2. The mixing index has been calculated on a cross section at 9.5 mm in the mixing channel

(0.5 mm from the outlet section), which ensures the mixture of fluids have replaced the fluid (water) that initially (t = 0 s) filled the mixing channel in the simulations. From the outcomes depicted in Fig. 2 it cannot be distinguished the trends in the mixing index with the variation of design parameters that define each case. Nevertheless, from Fig. 2 with Table 2, cases with f = 1 Hz gives higher mixing index than in other cases. Also, in cases with f = 1, 25 and 50 Hz, the mixing index is higher with $\phi = \pi/2$, while with f = 75 and 100 Hz this happens with the micropumps working in antiphase ($\phi = \pi$).

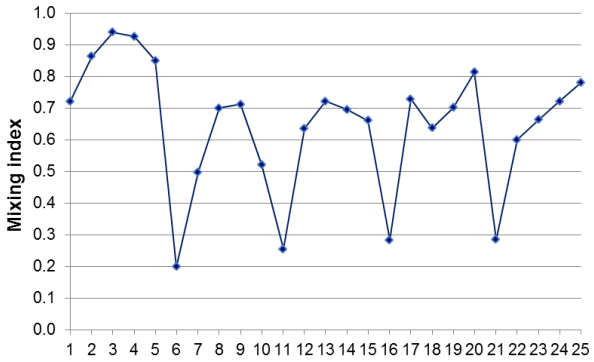

Fig. 2. Mixing index in the design cases of Table 2.

To evaluate the influence of the design parameters on the mixing index, it has been practiced a sensitivity analysis for which the variables were divided into design parameters and source of noise (noise factor). The set of simulations (25) given by the DOE can help to determine the design parameters that minimize the effect of noise factors on performance characteristics, using the loss function and Signal-to-Noise ratio (*S/N*) of the Taguchi method (Taguchi, 1987). When a response never has a negative value and its target value is ideally zero, these are referred to as smaller-the-better characteristics. Since the target response of the mixing index is ideally zero (see integrand in the square root of Eq. 4), the static Taguchi analysis for the problem with the smaller-the-better character is performed for having an initial estimation of optimum values of design variables. The Taguchi's *S/N* is a log function of the desired output which can serve as objective function to help in data analysis and in prediction of optimum results. To calculate the *S/N* on the basis of simulations results, the square of the standard deviation of concentration at a cross-section plane is calculated by

$$\sigma^2 = \frac{1}{n}\sum_{i=1}^{n}(c_i - c_\infty)^2 \tag{5}$$

where c_i is the concentration distribution of one of the fluids at the i_{th} cell of the mesh on the cross-section plane, c_∞ is the concentration of complete mixing (which equals 0.5 in this case) and n is the number of cells defined by the mesh on the plane. Then, the *S/N* with the smaller-the-better character can be evaluated by

$$\frac{S}{N} = -10\log\sigma^2 \tag{6}$$

The mixing index and the square of the standard deviation of the concentration are calculated at the same plane, so better mixing performance can be revealed by larger values of either the mixing index or the *S/N* ratio.

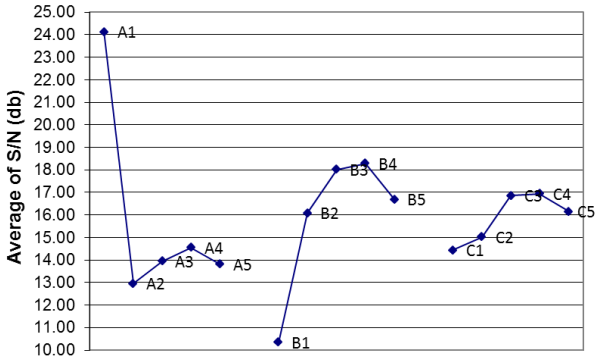

Fig. 3. Influence of design parameters on *S/N* ratio for a set of 25 models defined by the OA L_{25} (Table 2).

The results of *S/N* ratio are displayed in Fig. 3, where the positive slope of the curves indicates that increasing the value of the corresponding parameter results in a higher mixing index, and vice versa. From Fig. 3, the mixing index seems to be more sensitive to parameter A, the frequency of the pump actuators, for which the difference between the maximum and minimum of the average of the *S/N* ratios gives the highest value, followed by

parameters B and C in that order. Nevertheless, it is important to mention that the node A1 in Fig. 3 corresponds to f = 1 Hz in Table 1. This value is considerably lower than in the other cases (levels 2 to 5 in Table 1, i.e., 25 to 100 Hz), which implies that a much longer time, 100 s, was set for the simulation. Although one can see in Fig. 4 that the higher level of mixing in this case is achieved around 50 s, we can better compare the other cases whose total simulation times are between 1 s for f = 100 Hz and 4 s for f = 25 Hz.

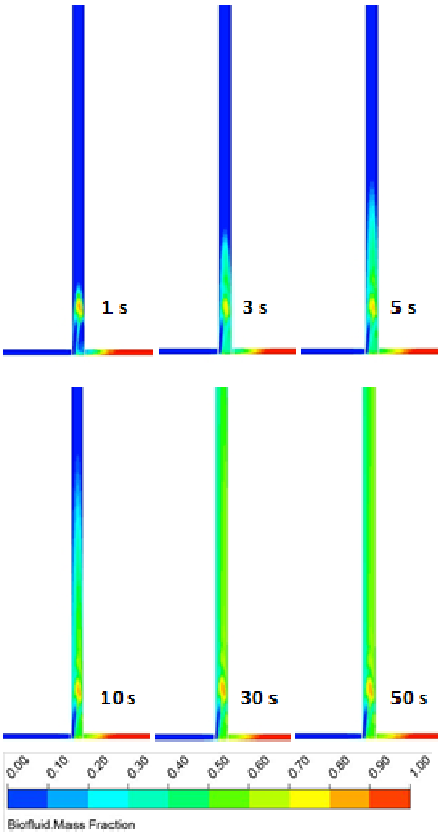

Fig. 4. Mass fraction contours on a mid-height plane at different times of design case 3 of Table 2 (f = 1 Hz, ϕ = π/2, θ = 180º), showing only 5 mm of mixing channel length.

This gives f = 75 Hz with design case 20 and f = 100 Hz with design case 25 as operation conditions to achieve higher mixing. In the same way, one can observe from Fig. 3 that the mixing index can be higher with ϕ = ¾π (or π/2) and θ = 210º (or 180º).

Other important physical variables in the microsystem are the pressure drop, shear strain and shear stress generated in the mixing channel. Fig. 5 shows the values of pressure drop in the design cases of Table 2.

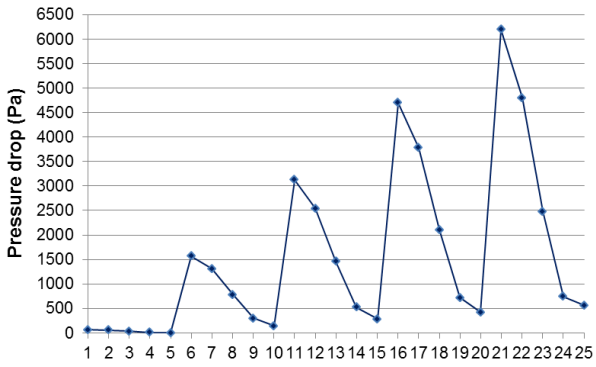

Fig. 5. Pressure drop in the design cases of Table 2.

The pressure drop in the mixing channel increases quasi-linearly with increasing frequency f. This increase is steeper with lower values of phase ϕ. The highest pressure drop in the system corresponds to the highest frequency applied, f = 100 Hz, and the lowest phase between the pump actuators, ϕ = π/36. The angle formed by the inlet channels at the junction, θ, in the range used in this study does not have effect on the level of pressure drop in the system.

Figs. 6 and 7 show the values of maximum shear strain rate and maximum shear stress respectively in the mixing channel of the design cases of Table 2. The variation of the levels and values of these physical variables among the design cases show same trends, indicating the shear stresses in the flow system are related to local gradient of velocity field.

The shear strain rate and shear stress in the system increase with increasing frequency f. Lower values of phase ϕ tends to make this increase steeper, but this is not exact for f >= 50 Hz. From this frequency value upwards, the effect of the geometry, i.e., the angle θ formed by the inlet channels, becomes relevant and the results show that shear strain and shear stress are lower for θ = 120º. This can be explained by a lower opposition to flow produced by this geometry, an actual Y-mixer, where both fluids flow into the mixing channel with the minimum change of direction (60º) among the design cases and, consequently, lower velocity gradients in the device volume.

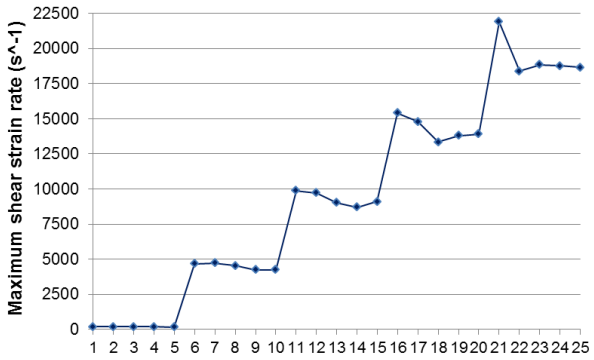

Fig. 6. Maximum shear strain in the design cases of Table 2.

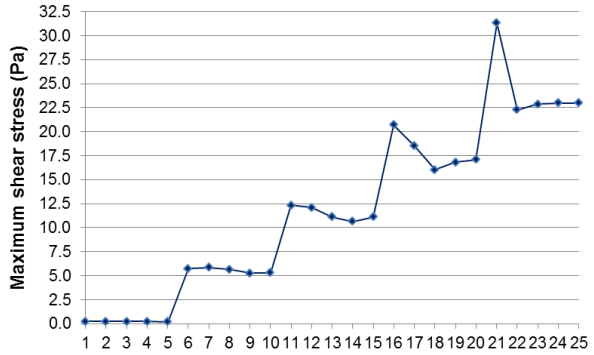

Fig. 7. Maximum shear stress in the design cases of Table 2.

As indicated previously, the results presented and analyzed correspond to the total time of the transient simulations, which is between 1 s (f = 100 Hz) and 100 s (f = 1 Hz), i.e., 100 system cycles. The evaluation of the design performance should also include the time required by the design to achieve the highest level of mixing index and the channel length at which this occurs.

This evaluation can be seen in the example given in Figs. 8 and 9. This additional design case has been prepared taking into account the results obtained in the 25 DOE cases. This microsystem case corresponds to parameters f = 100 Hz, $\phi = \pi$ and θ= 180º. Although design cases with f = 1 Hz give higher values of mixing, they require longer times to achieve them. For other values of f in this study, the level of mixing is approximately of the same order, with mixing increasing consistently with increasing ϕ in the case of f = 100 Hz. Although the pressure drop in the system is higher for this value of f, it can be lowered to a feasible practical value of about 500 Pa when the micropumps work in antiphase mode ($\phi = \pi$). The maximum shear strain rate and shear stress in the system for f = 100 Hz do not change much in magnitude with θ, with the exception of θ= 240º that increases them considerably. Therefore, the typical T-mixer channel (θ= 180º) was chosen to model the additional design case.

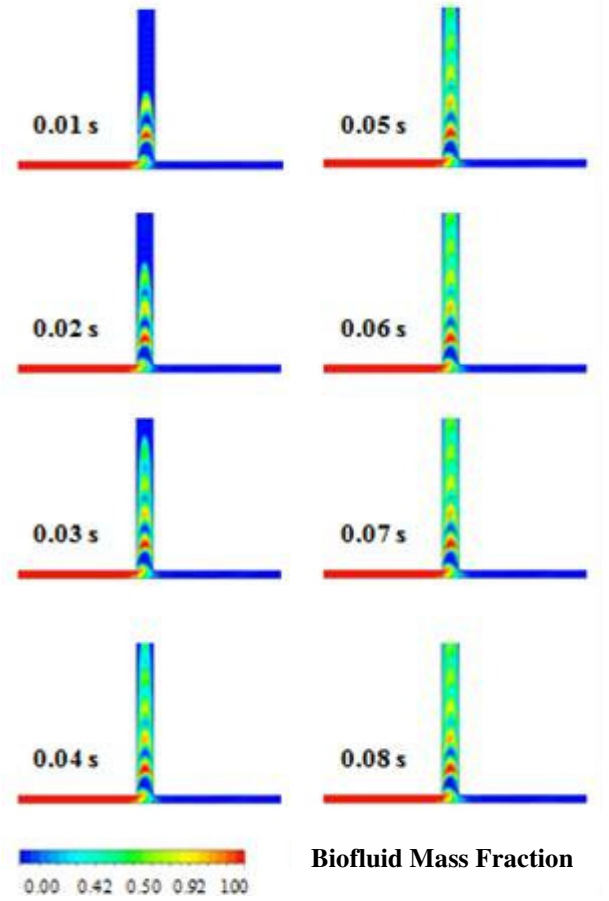

Fig. 8. Mass fraction contours on a mid-height plane at different times (case: f = 100 Hz, $\phi = \pi$, θ= 180º)), showing only 1.3 mm of mixing channel length.

Fig. 8 shows the variation of the mass fraction on a mid-height plane in the mixer component. One can see clearly that the mixing level in the first part of the channel increases quickly in just 0.08 s although it has not reached yet a steady regime. This can be observed more clearly in Fig. 8 which shows the variation of mixing index within the total simulation time of 1 s calculated at several cross-section planes in the mixing channel. A maximum steady value of mixing index of 0.92 is achieved at 3 mm in about 0.45 s. The same level of mixing but at 8 mm can only be achieved in

about 0.95 s. This demonstrates that this microsystem can achieve the same steady level of mixing in a channel of 3 or 8 mm length in conservative times of 0.5 and 1 s respectively. This information is relevant since that a shorter channel implies lower level of pressure drop which favours the system performance.

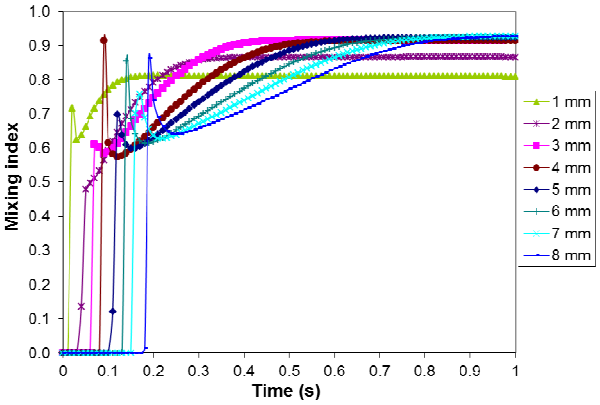

Fig. 9. Change of mixing index at different cross- sections of the mixing channel (case: f = 100 Hz, $\phi = \pi$, θ = 180º).

Conclusions

Numerical simulations have been used to investigate flow and mixing in a feasible microsystem composed by two valveless micropumps arranged in parallel and a typical T-type micromixer. The design cases modelled for a parametric study were defined with a DOE Taguchi's Orthogonal Array. The parameters include two operating conditions of the micropumps, frequency of actuators f and phase ϕ between them, and one geometric feature of the T-mixer, the angle θ formed by the inlet channels at the junction.

It has been found that the microsystem enhances mixing at different operating conditions, from which the more efficient have been analyzed and indicated. It has the advantage of incorporating the simplest planar geometry for the mixer component, the T-type mixer, without requiring additional inlet channels or structures in the mixing channel. Mixing occurs from the confluence region so an additional volume is not required, what is desirable for the loading of liquids without air bubbles in channels. The work conditions in this study produce fluctuating flow rates with peaks of 3.23E-03 to 3.60 µL/s (see Fig. 10) and Reynolds numbers of 0.03 to 30 in the mixing channel respectively. The viability of the system to work with cells was examined by calculating the maximum shear stress and strain rate, in view that the laminar shear stresses for long duration do not cause cell membrane disruption.

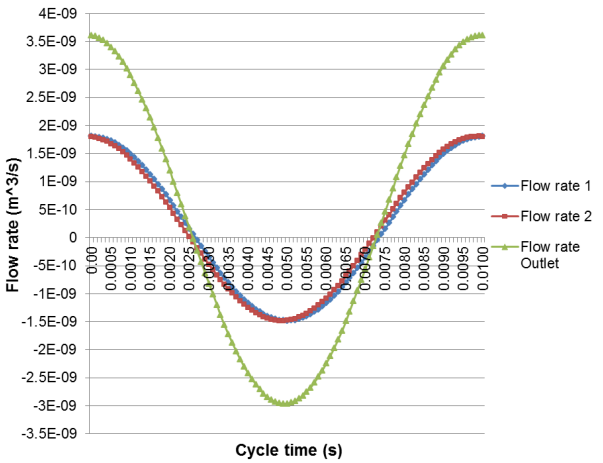

Fig. 10. Flow rate in the inlet and mixing channels of the micromixer in a representative work cycle of design case 21 of Table 2 (f = 100 Hz, $\phi = \pi/36$, θ = 240º).

References

ANSYS Inc., 2010. CFX 13.0 User Manual.

ANSYS Inc., 2010. ICEM CFD 13.0 User Manual.

Azarbadegan, A., Cortes-Quiroz, C.A., Eames, I., Zangeneh M., 2010. Analysis of double-chamber parallel valveless micropumps. Microfluid. Nanofluid. 9, 171-180.

Azarbadegan, A., Eames, I., Wojcik, A., Cortes-Quiroz, C.A., Suen, W., 2013. Combination rules for multichamber valveless micropumps. J. Microelectromech. Syst. 22 (5), 1133-1139.

Chen, C-K., Cho, C-C., 2008. A combined active/passive scheme for enhancing the mixing efficiency of microfluidic devices. Chem. Eng. Sci. 63, 3081-3087.

Cortes-Quiroz, C.A., Azarbadegan, A., Zangeneh, M., Goto, A., 2010. Analysis and multi-criteria design optimization of geometric characteristics of grooved micromixers. Chem. Eng. J. 160, 852-864.

Hessel, V., Lowe, H., Schonfeld, F., 2005. Micromixers: a review on passive and active mixing principles. Chem. Eng. Sci. 60, 2479-2501.

Glasgow, I., Aubry, N., 2003. Enhancement of microfluidic mixing using time pulsing. Lab Chip 3, 114-120.

Miranda, J.M., Oliveira, H., Teixeira, J.A., Vicente A.A., Correia, J.H., Minas, G., 2010. Numerical study of micromixing combining alternate flow and obstacles. Int. Comms. Heat Mass Transf. 37, 581-586.

Nguyen N.T., Wu Z., 2005. Micromixers - a review. J. Micromech. Microeng. 15, R1-R16.

Niu X., Lee Y-K., 2003. Efficient spatial-temporal chaotic mixing in microchannels. J. Micromech. Microeng. 13, 454-462.

Taguchi G., 1987. Systems of Experimental Design, vols. 1 and 2, Kraus International, New York.